



HAL
open science

Non-isocyanate polyurethane nanoprecipitation: Toward an optimized preparation of poly(hydroxy)urethane nanoparticles

T. Quérette, C. Bordes, N. Sintès-Zydowicz

► To cite this version:

T. Quérette, C. Bordes, N. Sintès-Zydowicz. Non-isocyanate polyurethane nanoprecipitation: Toward an optimized preparation of poly(hydroxy)urethane nanoparticles. *Colloids and Surfaces A: Physicochemical and Engineering Aspects*, 2019, 589, pp.124371. 10.1016/j.colsurfa.2019.124371 . hal-02456016

HAL Id: hal-02456016

<https://hal.science/hal-02456016>

Submitted on 7 Mar 2022

HAL is a multi-disciplinary open access archive for the deposit and dissemination of scientific research documents, whether they are published or not. The documents may come from teaching and research institutions in France or abroad, or from public or private research centers.

L'archive ouverte pluridisciplinaire **HAL**, est destinée au dépôt et à la diffusion de documents scientifiques de niveau recherche, publiés ou non, émanant des établissements d'enseignement et de recherche français ou étrangers, des laboratoires publics ou privés.



Distributed under a Creative Commons Attribution - NonCommercial 4.0 International License

Non-Isocyanate Polyurethane Nanoprecipitation: toward an Optimized Preparation of Poly(hydroxy)urethane Nanoparticles

T. Quérette^{a,c}, C. Bordes^b, N. Sintès-Zydowicz^c

^a University of Lyon, IMP@INSA, UMR5223, 17, Av. Jean Capelle, 69621 Villeurbanne Cedex

^b University of Lyon, Université Claude Bernard Lyon 1, Laboratoire d'Automatique, de Génie des Procédés et de Génie Pharmaceutique, UMR CNRS 5007, Villeurbanne, France

^c University of Lyon, Université Claude Bernard Lyon 1, IMP@Lyon1, UMR5223, 15, Bd. Latarjet, 69622 Villeurbanne Cedex

Keywords: poly(hydroxy)urethane, nanoprecipitation, nanoparticles, full-factorial matrix

Abstract

This study describes the influence of different parameters on the production of monodisperse and stable poly(hydroxy)urethane (PHU) nanoparticles with a size inferior to 100 nm by nanoprecipitation. DMSO and SDS were used as polymer solvent and surfactant respectively. Nanosuspensions were characterized by dynamic light scattering (DLS) and cryo-transmission electronic microscopy (cryo-TEM). A full-factorial design was employed to study the main effects and interaction effects of three independent variables – polymer concentration in the organic phase (X_1), water volume (X_2) and surfactant concentration in the aqueous phase (X_3) – on two responses – particle size (Y_1) and size distribution (Y_2). The results allowed to determine the experimental conditions favouring the smallest diameter or the narrowest size distribution. The critical micellar concentration value of SDS in various water-solvent mixtures helped to highlight the role of the surfactant in the PHU nanosuspension characteristics and stability. The results showed that the use of surfactant was mandatory for nanosuspension stabilization, but the presence of numerous surfactant micelles induced nanoparticle aggregation. Finally, the ageing study evidenced that nanosuspensions with the lowest size distribution were the most stable over time.

Introduction

During the last decades, polymer nanoparticles have attracted growing interest because of their potential use as active agent delivery in various fields of application such as cosmetics[1], agrochemistry[2] and pharmaceuticals[3]. Various methods have been developed to prepare nanoparticles: solvent evaporation[4], salting-out[5], emulsion-diffusion[6], rapid expansion of supercritical fluid[7], temperature[8] or pH[9] modification, layer-by-layer deposition[10] and nanoprecipitation[11]. The latter offers many advantages: this straightforward and reproducible method[12] guarantees the absence of monomer, oligomer or other reactant trapped in the nanoparticles[13]. Moreover, the spontaneous formation of nanoparticles does not require an expensive mechanical energy input[14].

The nanoprecipitation technique consists in the dropwise addition of an organic phase (i.e. a preformed water-insoluble polymer dissolved in a completely water-miscible organic solvent) to an aqueous phase[15]. The simultaneous water/organic solvent inter-diffusion and polymer precipitation may lead to the formation of particles in the 50-300 nm range with a narrow size distribution[16]. A large number of parameters have already been investigated because of their potential influence on the properties of the final nanoparticle suspension[17, 18] and theoretical models have been deduced from these results[12, 19]. In parallel, several designs of experiments have been carried out to refine the parameter study[20-23]. However, given the variety of the nanoprecipitation systems studied, it is not possible to discern a general trend from these analyses.

Various synthetic polymers have already been nanoprecipitated successfully (PLA, PCL, PLGA, PLA-PEG, PCL-PEG, PLGA-PEG, PNIPAm, PMMA)[15]. Very few studies have focused on polyurethane (PU) nanoprecipitation[24, 25] although the good blood compatibility[26] and biodegradability[27] of PU. PU nanoparticles have been mainly

prepared by in situ polyaddition in miniemulsion[28-30]. The major drawback of traditional PU is the toxicity of the isocyanate monomers involved in the polymer synthesis [31, 32]. Moreover, the synthesis of isocyanate requires phosgene, a noxious gas [33], to convert amine into isocyanate. To overcome this obstacle, various synthesis routes have been proposed to prepare non-isocyanate polyurethane [34]. The greenest and most straightforward way to synthesize non-isocyanate polyurethanes is the polyaddition of bis-5(cyclic carbonate)s and diamines[35]. The resulting polymer is called a poly(hydroxy)urethane (PHU) because of the presence of primary and secondary hydroxyl groups hanging off the main polymer chain that offers the possibility to post-functionalize the hydroxyl groups with chemical or biological functionalities [36, 37]. However, the low reactivity of diamines toward bis-5(cyclic carbonate)s [38] does not allow to prepare PHU nanoparticles by in situ miniemulsion interfacial polymerization as it is the case for PU nanoparticles. We recently demonstrated that the nanoprecipitation technique was suitable for the preparation of PHU nanoparticles: PHU nanosuspensions were prepared using DMSO ($d_{\text{moy}} = 140$ nm, PDI = 0.14) or ethanol ($d_{\text{moy}} = 90$ nm, PDI = 0.22) as the organic solvent [39]. Nevertheless, particle destabilization was observed after a couple of weeks, suggesting that the presence of a surfactant in the aqueous phase was required to improve the stability of the nanoparticles over time.

The aim of this study was to determine the parameters that govern the size distribution of PHU nanoparticles prepared by nanoprecipitation. For this purpose, the effect of polymer concentration, water volume and surfactant concentration on both the mean size and the polydispersity index of the resulting nanoparticles was investigated by the means of a two-level full factorial design. Unlike the ‘one-factor-at-a-time’ approach, the factorial design approach allows to investigate interactions between the parameters studied[40-42] and may allow to obtain response surfaces that provide continuous response prediction in the defined experimental domain. Response surface methodology is widely used to optimize particle

formulation processes often with the objective of minimizing both particle mean size and PDI values [23, 43, 44]. The surfactant concentration and its effect on micelles formation were particularly examined. Finally, we attempted to connect the nanosuspension stability over time with the initial characteristics of PHU nanoparticles.

Experimental section

Materials

Dimethylsulfoxide (DMSO) (99.8 %, Carlo Erba), and sodium dodecyl sulfate (SDS) (≥ 98.5 %, Sigma-Aldrich) were purchased and used as received. Permuted water was prepared from tap water filtrated through a cation and anion filter system. Hereafter in this article, permuted water will be mentioned as water. Poly(hydroxy)urethane (PHU) synthesis, purification and characterization are described in a previous study [39]. PHU main characteristics are as follows: $\bar{M}_n = 12\,900$ g/mol, $\bar{M}_w = 30\,000$ g/mol, $T_d = 210^\circ\text{C}$, $T_g = -7^\circ\text{C}$. PHU molar mass, degradation temperature and glass transition temperature were determined by gel permeation chromatography (DMSO / 0.1 wt% NaNO_3 , universal calibration), thermogravimetric analysis and differential scanning calorimetry respectively [39].

PHU nanoprecipitation

In a typical procedure, 25 mg of polymer were dissolved into 25 ml of DMSO (one night at room temperature) to prepare the organic phase. 360 mg of SDS were dissolved into 50 ml of water to prepare the aqueous phase. At 24°C , the organic phase was filled up in a plastic syringe (BD Plastipak, H 851 ES, 50 ml) and added dropwise (35 ml/h, using a syringe pump) in the aqueous phase under stirring (500 rpm). 50 ml of the nanosuspension were collected in a vial. The following parameters were fixed for all the experiments: system temperature, stirring rate, type of needle, addition rate, distance between the tip of the needle and the surface of the aqueous phase. The same glassware, laboratory equipment and fume hood were

used for every experiment. The vials used to collect the nanosuspension after nanoprecipitation were washed with ethanol and acetone and dried in an oven prior to their use.

Design of experiments

In order to investigate the nanoprecipitation technique, three experimental factors were studied by the means of a design of experiments: the concentration of polymer in the organic solution (X_1), the volume of water (X_2) and the concentration of SDS in the aqueous phase (X_3). They are presented with their coded levels in Table 1. More precisely, the main effects of each factor as well as their interaction effects on the nanoparticle size distribution were investigated by carrying out eight runs that were determined by a 2^3 full factorial design (Table 2) [45]. Two experimental responses were measured by dynamic light scattering (DLS) analyses: the polydispersity index (PDI) (Y_1) and the mean particle size (d) (Y_2). The responses were modelled by a three degree polynomial as follows:

$$\hat{Y} = b_0 + b_1X_1 + b_2X_2 + b_3X_3 + b_{12}X_1X_2 + b_{13}X_1X_3 + b_{23}X_2X_3 + b_{123}X_1X_2X_3 \quad (1)$$

where \hat{Y} is the predicted response, b_0 is the intercept, the coefficient b_i is the main effect of the coded factor X_i , the coefficients b_{ij} and b_{123} are the two-factors and three-factors interaction effects, respectively. The coefficients of Equation 1 were determined by ordinary least square regression using the eight design points (Experiments 1 to 8 in Table 2). Four replicated experiments were also carried out at the centre of the experimental domain and used as check points in order to evaluate the predictive performance of the developed models (Experiments A to D in Table 2). Multiple linear regression analyses were performed using NEMRODW® software (LPRAI, Marseille, France).

Ageing study

After their preparation, the suspensions were stored in vials at 24°C. 17, 27, 47 and 214 days after their preparation, samples were submitted to DLS measurements to observe the evolution of nanoparticle size and size distribution over time.

PHU nanoparticle characterization

SDS critical micellar concentration

To better understand the behaviour of SDS in the dispersant medium and its role on the nanoparticle formation and stability, SDS critical micellar concentration (CMC) was determined in 1:2, 1:4 and 1:6 DMSO/water solutions by measuring the surface tension of solutions with different SDS concentrations using a K100 tensiometer from Krüss and a Wilhelmy plate. SDS/solvent/water stock solutions were filtrated (0.45 µm cellulose ester filter), and the dilutions were creamed with Joseph paper before use. Every tension surface measurement was repeated three times. Before every measurement, the Wilhelmy plate was cleaned with acetone, dried with Joseph paper and heated with a blowtorch.

Dynamic light scattering (DLS)

Less than an hour after every sample preparation, nanoparticle size distributions were determined by dynamic light scattering (DLS) on a Nanosizer ZS (Malvern Instruments) with a detection angle of 173°. The correlation decay function was analysed by the cumulant method to determine the z-average diameter and polydispersity index (PDI). With a PDI inferior or equal to 0.2, the nanoparticle size (d) corresponded to the z-average diameter (z-ave). With a PDI superior to 0.2, the nanoparticle size corresponded to the mean diameter of the nanoparticle population (d_{moy}). For every analysis, 1 ml of the sample was analysed as such in a disposable cuvette at 24.0 ± 0.1 °C. Depending on the proportion of DMSO and water

in the nanosuspension, specific values of the dynamic viscosity, refractive index and dielectric constant were entered for the DLS analysis [46, 47] (table S1).

Cryo-transmission electron microscopy (cryo-TEM)

Cryo-transmission electron microscopy (cryo-TEM) observations were performed under a Philips CM 120 transmission electron microscope operating with low-dose scanning under reduced pressure. For every sample, a small drop (ca. 5 μ L) of 0.5% (w/v) particle suspension was pipetted onto an advanced holey carbon film (Quantifoil, EMS) coated copper grid. The excess of sample was removed by quick blotting with filter paper leaving a thin spanned film of the sample. The grid was immediately vitrified by being plunged into liquid ethane cooled by liquid nitrogen (Cryoplunge, Orsay University). The sample was transferred into liquid nitrogen and inserted into a cold cryo-holder (Gatan). The holder was quickly transferred into the vacuum column of TEM microscope maintained at liquid nitrogen temperature. An accelerating voltage of 120 kV was used for the observations.

Results and discussion

SDS critical micellar concentration in water and DMSO/water solutions

In our previous study [39], we observed that size and size distribution of PHU nanoparticles remained stable the first 15 days after their preparation by nanoprecipitation, and significantly increased between 15 and 28 days. Then we aimed to improve the stability of the PHU NPs by the use of a surfactant. SDS was selected for the current study because this surfactant has successfully stabilized nanoparticles of PU with a very similar chemical structure to PHU [48]. In addition, the efficacy of SDS compared to non-ionic surfactants is ensured by the electrostatic barrier that it provides to the nanoparticles.

If surfactant may improve the stability of nanoparticles prepared by nanoprecipitation, its concentration must be carefully selected. In most nanoprecipitation protocols, the

concentration of SDS present in the aqueous phase does not exceed 1 mmol/L [22, 49, 50]. Bibette *et al.* reported that an excessive quantity of SDS causes the destabilization of a nanosuspension [51]. Indeed, numerous micelles of SDS apply entropic depletion forces on the nanoparticles and thus induce their aggregation. Thus, keeping track of the quantity of SDS micelles in our samples appeared to be mandatory to avoid destabilization phenomenon.

The critical micellar concentration (CMC) is defined as the concentration of surfactant above which micelles form. The CMC of SDS in permuted water has been reported in the literature and ranges from 6 [52] to 8 [53] mmol/l at 22–25°C. The CMC of SDS in binary DMSO/water mixtures [54, 55] (ranging from 6.5 to 9.5 mmol/l with 0 to 30 %V of DMSO [55]) is less reported. This information is crucial here since PHU nanoparticles once prepared by nanoprecipitation are suspended in DMSO/water mixtures.

Surface tension measurements were performed in permuted water and binary DMSO/water mixtures at different SDS concentrations. The surface tension was plotted versus the logarithm of the SDS concentration to determine the value of the CMC. The CMC of SDS determined in permuted water was equal to 6.1 mmol/l (Figure S1). The values of the CMC of SDS determined in DMSO/water mixtures were equal to 6.7, 7.8 and 10.6 mmol/l for DMSO/water ratios equal to 1:6, 1:4 and 1:2 respectively (Figure S2). The CMC linearly increased with the increase of DMSO amount as it was reported by Harutyunyan and Markarian [54].

According to the Rosen classification, DMSO is a class II organic additive [56]: DMSO is capable of forming hydrates with water and SDS [57, 58], inducing the decrease of the quantity of SDS available to form micelles. Furthermore, the presence of DMSO induces the decrease of the solubility parameter δ and dielectric constant ϵ of the aqueous solution. Consequently, the increase of surfactant solubility [59] and head-to-head electrostatic repulsions [56] may favour the increase of the CMC of SDS.

Design of experiments (DOE)

Experimental domain

In this study, three parameters were investigated because of their potential impact on nanoparticle polydispersity (Y_1) and mean size (Y_2): PHU concentration in the organic phase (X_1), water volume (X_2) and SDS concentration in the aqueous phase (X_3).

The effect of the polymer concentration has been widely investigated [12, 60, 61]. Most of the studies report that size and polydispersity of particles increase with polymer concentration. The increase of the organic phase viscosity induced by the increase of the polymer concentration favors the particle growth step [62, 63]. Thus, working in the dilute regime [64] is recommended to form small size nanoparticles.

Water volume may impact the rate of solvent diffusion. A study from Fonseca et al. reports the decrease of particle size by increasing the water volume [65] whereas no significant impact on the nanosuspension is reported by other authors [18, 62]. These contradictory results may be explained by differences of stirring speed [66] and organic phase addition rate [18] values because these two parameters also influence solvent diffusion.

The role of the surfactant is to prevent nanoparticle destabilization (i.e. aggregation, coalescence or Ostwald ripening) [16]. Moreover, different authors have observed that the increase of surfactant concentration in the aqueous phase induces the decrease of the nanoparticle size and size polydispersity [23, 66-68]. However, some studies report the preparation of small and monodisperse nanoparticles by nanoprecipitation without surfactant [69, 70]. Other parameters could potentially affect the process (polymer molar mass [18], temperature, organic and aqueous phase mixing time – using a confined impinging jet reactor for instance [12]), but here we decided to focus on the three parameters presented above.

The range of PHU concentration (1 to 5 g/l), water volume (50 to 150 ml) and SDS concentration (0.0 to 25.0 mmol/l) was selected according to the literature [15]. Regarding the studied responses, the polydispersity of the particle size distribution (Y_1) is an important NPs characteristic since a low PDI enables the long-term stability of the nanosuspension [14, 71]. The second selected response, the particle mean size (Y_2), is also a crucial characteristic which depends on the nanoprecipitation process conditions [12, 14, 72].

As described in the experimental section, a full factorial design 2^3 was used to determine the influence of the main effects and the interaction effects between the three selected experimental factors on the size distribution of PHU nanoparticles. The acquired knowledge should lead to determine the operating conditions suitable for the obtaining of monodisperse and minimal sized NPs by nanoprecipitation of PHU.

Results

Nanoparticle mean size (Y_2) and PDI (Y_1) were measured by DLS for each sample (Table 1). Depending on the operating conditions, results indicated significant evolution of both the mean size ranging from 55 up to 179 nm and the polydispersity index from 0.1 to 0.52. To well assess the robustness of the nanoprecipitation process and to determine reliable estimations of the experimental variances for Y_1 and Y_2 , we repeated several runs in addition to the four centre points (Table 1). Runs 3, 5 and 6 were repeated because the corresponding samples displayed a PDI and a particle size inferior to 0.2 and 100 nm respectively. These values appeared especially interesting in the frame of the study. Run 4, corresponding to nanoparticles characterized by a monomodal but large size distribution, was also repeated for comparison purposes.

All these genuine repeats (4 centre points, the triplicates of runs 3, 4 and 6 and the duplicated run 5) allowed to reliably estimate with 10 degrees of freedom the experimental standard deviations $\sigma_1 = 0.024$ and $\sigma_2 = 13$ nm for Y_1 and Y_2 , respectively. According to these

estimations, the corresponding 95% confidence intervals were determined: $Y_1 \pm 0.05$ and $Y_2 \pm 25$ nm.

Due to the specific structure of the full factorial design, the estimations of the coefficients of the postulated models (Equation 1) are characterized by the same standard deviation which is equal to $\sigma_{b_i(Y_1)} = \frac{\sigma_1}{\sqrt{N}} \sim 0.01$ for Y_1 and $\sigma_{b_i(Y_2)} = \frac{\sigma_2}{\sqrt{N}} \sim 4.3$ for Y_2 (with N the number of the designed points, $N = 8$)[40]. The 95% confidence interval of the coefficients denoted Δb_i was then determined and is expressed as:

$$\Delta b_i = t_{theo} \times \sigma_{b_i} \quad (2)$$

Where t_{theo} is the theoretical value of the Student t statistic which is equal to 2.22 [73] with a risk of 0.05 and ten degrees of freedom.

The 95% confidence interval of the coefficients ($\Delta b_{i(Y_1)} = 0.02$ and $\Delta b_{i(Y_2)} = 9.5$) inform about the statistical significance of each effect in the models: a coefficient b_i larger in absolute value than Δb_i indicates a significant effect (at the 0.05 level) of the factor i on the studied response.

The main effects (b_1, b_2, b_3), 2-factor interaction (b_{12}, b_{13}, b_{23}) and 3-factor interaction (b_{123}) effects were calculated by least squares linear regression and are represented with their 95% confidence intervals in Figures 1 and 4 for the responses Y_1 and Y_2 , respectively.

Analysis of the DOE results obtained for the response Y_1 (PDI)

Results highlighted five significant effects on the PDI: the main effects of PHU concentration in the organic phase (X_1) and the water volume (X_2) as well as all the interactions involving the SDS concentration (X_3). According to Eq.1, the PDI may be expressed as:

$$\hat{Y}_1 = 0,24 - 0,03 \times X_1 + 0,04 \times X_2 - 0,06 \times X_1 \times X_3 + 0,07 \times X_2 \times X_3 - 0,05 \times X_1 \times X_2 \times X_3 \quad (3)$$

The positive coefficient of X_2 means that the PDI increased when the water volume ranged from 50 to 150 mL. Inversely, due to its negative coefficient, the evolution of PHU concentration from 1 to 5 g/L caused a PDI decrease. According to these results, the minimal value of \hat{Y}_1 should be obtained with $X_1 = +1$ ([PHU] = 5 g/l) and $X_2 = -1$ ($V_w = 50$ ml).

The significant two-factor interactions X_1X_3 and X_2X_3 are presented in Figures 2a and b, respectively. Figure 2a shows that the effect of the water volume depended on the SDS concentration: without SDS it was slightly negative while it appeared positive and intense at 25 mM SDS. The lowest PDI (0.12) was obtained for $X_2 = -1$ ($V_w = 50$ ml) and $X_3 = +1$ ([SDS] = 25.0 mM) while the highest PDI (0.36) was obtained for $X_2 = +1$ ($V_w = 150$ ml) and $X_3 = +1$ ([SDS] = 25.0 mM) (Figure 2a). The effect of the PHU concentration also depended on the SDS concentration since without SDS it was not significant and at 25 mM SDS it significantly decreased the PDI from 0.33 to 0.15 (Figure 2b). The lowest PDI (0.15) was obtained for $X_1 = +1$ ([PHU] = 5 g/l) and $X_3 = +1$ ([SDS] = 25.0 mM) while the highest PDI (0.33) was obtained for $X_1 = -1$ ([PHU] = 1 g/l) and $X_3 = +1$ ([SDS] = 25.0 mM) (Figure 2b).

Regarding the 3-factor interaction effect (Figure 3a and 3b), results indicated that the interaction between the concentration of PHU and the water volume depended on the SDS concentration. The lowest PDI (0.10) was obtained for $X_1 = +1$ ([PHU] = 5 g/l), $X_2 = -1$ ($V_w = 50$ ml) and $X_3 = +1$ ([SDS] = 25.0 mM) while the highest PDI (0.52) was obtained for $X_1 = -1$ ([PHU] = 1 g/l), $X_2 = +1$ ($V_w = 150$ ml) and $X_3 = +1$ ([SDS] = 25.0 mM).

All these results obtained from the analysis of the significant main effects and interaction effects were consistent and evidenced that the most monodisperse size distribution should be obtained by using a PHU concentration of 5 g/l, a water volume of 50 ml and a SDS concentration of 25.0 mM. These conclusions are in accordance with the experimental results since the corresponding experiment (run 6) led to a nanosuspension characterized by small mean diameter 88 nm and PDI 0.1.

Analysis of the DOE results obtained for response Y₂ (particle mean size)

The regression model calculated for Y₂ was the following:

$$\hat{Y}_2 = 101 + 12 \times X_2 - 15 \times X_1 \times X_2 - 11 \times X_1 \times X_3 + 18 \times X_2 \times X_3 - 17 \times X_1 \times X_2 \times X_3 \quad (4)$$

The regression coefficients are also displayed in Figure 4. The most significant effects were the two-factor interactions X₁X₂ and X₂X₃ as well as the three-factor interaction. The two-way diagrams corresponding to X₁X₂ and X₂X₃ interactions (Figures 5a and b) show that the effect of the water volume on the nanoparticle mean size depends on the SDS and PHU concentrations, respectively. Regarding the interaction between the water volume and SDS concentration (Figure 5a), the lowest particle mean size (71 nm) was obtained for X₂ = -1 (V_w = 50 ml) and X₃ = +1 ([SDS] = 25.0 mM) while the highest particle mean size (130 nm) was obtained for X₂ = +1 (V_w = 150 ml) and X₃ = +1 ([SDS] = 25.0 mM). Concerning the interaction effect between the PHU concentration and the water volume (Figure 5b), the lowest particle size (79 nm) was obtained with X₁ = -1 ([PHU] = 1 g/l) and X₂ = -1 (V_w = 50 ml) while the highest particle size (130 nm) was obtained with X₁ = -1 ([PHU] = 1 g/l) and X₂ = +1 (V_w = 150 ml) (Figure 5b). Nevertheless, a low particle size (91 nm) was also obtained with X₁ = +1 ([PHU] = 5 g/l) and X₂ = +1 (V_w = 150 ml).

To interpret the 3-factor interaction effect, the interaction between the water volume and the PHU concentration is represented in Figure 6 for the two studied levels of the SDS concentration: this indicates that the interaction effect X₁X₂ depends on the SDS amount. Moreover, the lowest particle size (55 nm) was obtained for X₁ = -1 ([PHU] = 1 g/l), X₂ = -1 (V_w = 50 ml) and X₃ = +1 ([SDS] = 25.0 mM) while the highest particle size (179 nm) was obtained for X₁ = -1 ([PHU] = 1 g/l), X₂ = +1 (V_w = 150 ml) and X₃ = +1 ([SDS] = 25.0 mM). These results clearly pointed out the important influence of the water volume at a low concentration of PHU in the presence of SDS.

A low significance was also observed for the main effect of the water volume (X_2) and the two-factor interaction X_1X_3 (results not shown). The main effects of X_1 and X_3 as well as the interaction between the PHU concentration and SDS concentration did not significantly affect the particle mean size.

Centre points were carried out and used as check points in order to assess the predictive performance of the developed models (Eq. 3 and 4).

At the centre of the experimental domain ($X_i = 0$, i.e. [PHU] = 3 g/l, $V_w = 100$ ml and [SDS] = 12.5 mM), the models predicted a nanosuspension characterized by a PDI of 0.24 and a mean size of 101 nm, while we experimentally obtained nanoparticles with a mean size of ~94 nm and a PDI of ~0.13 (runs A to D). The corresponding residuals in absolute value were equal to 0.11 for Y1 and 7 nm for Y2. According to the 95% confidence intervals of the responses ($Y1 \pm 0.05$ and $Y2 \pm 25$ nm), these results indicated that only the Y2 model (Eq. 4) may be used for prediction purpose in the whole experimental domain. Using all the repeated runs, the fitting quality of the model was assessed by i) ANOVA results that indicated the high significance of the model ($p\text{-value} < 0.05$) and ii) the R^2 -adjusted coefficient ~0.92. Once validated, the model was used to visualize the response surfaces [74] using the software MODDE® (Umetrics, Sartorius Stedim Biotech). Figures 7 a, b and c present the contour plot of the response surface for Y2 at [SDS] = 0, 12.5 and 25.0 mM, respectively.

In the absence of SDS, no significant evolution of the particle mean size was observed by varying the PHU concentration and the water volume since one observed a negligible variation between 85 nm (low PHU concentration and high water volume) and 105 nm (high PHU concentration and low water volume) (Figure 7a).

In the presence of SDS, similar contour plots have been obtained, regardless of the SDS concentration (Figure 7b and 7c). The lowest values of particle mean size should be obtained with both low PHU concentration and water volume: a mean size of 75 nm and 80 nm were

predicted by using an SDS concentration of 25.0 mmol/l and 12.5 mmol/l, respectively. The particle mean size was high with a low PHU concentration and a high water volume: the model predicted a mean size of 160 nm at 25.0 mmol/l SDS and 125 nm at 12.5 mmol/l SDS. Water volume exhibited a high effect on particle mean size when PHU concentration was below 2.5 g/l, but its influence decreased as the PHU concentration increased. At a high PHU concentration (5 g/l), the effect of water volume on particle mean size was negligible since the mean size ranged between 90 and 100 nm. Comparing Figures 7b and 7c reveals that the higher SDS concentration, the higher the influence of water volume on particle size when PHU concentration is low: particle mean size varied from 80 and 125 nm when water volume increased from 50 to 150 ml for a SDS concentration of 12.5 mmol/l, and from 75 to 160 nm for a SDS concentration equal to 25.0 mmol/l.

Discussions

Influence of the amount of surfactant

We aimed to compare the size distribution of PHU NPs with and without surfactant. To the best of our knowledge, such a study was not reported in the literature.

- Surfactant-free samples

Samples 1, 2 and 4 – prepared without SDS – displayed a unimodal but large size distribution (Figure 8, sample 1). Although nanoparticles were monodisperse in sample 3 (PDI = 0.15, z-ave = 87 nm), repetitions 3' (z-ave = 88 nm, PDI = 0.20) and 3'' (z-ave = 118 nm, PDI = 0.25) followed the general trend displaying a unimodal but large size distribution.

These results indicated that nanoparticles underwent aggregation or coalescence in the absence of surfactant. Moreover, it could be assumed that DMSO could diffuse into nanoparticles, inducing particle swelling.

Consequently, the presence of SDS appeared to be necessary in order to prevent particle destabilization right after their preparation by nanoprecipitation.

- Samples with a high amount of surfactant

Samples 7 and 8 were prepared with the same volume of water and concentration of SDS but with different concentrations of PHU. PHU concentration was 5 times higher in sample 8 than in sample 7. Water volume and SDS concentration were at the highest level ($X_2 = +1 = 150$ ml, $X_3 = +1 = 25.0$ mmol/l) inducing the highest quantity of SDS ($m(\text{SDS}) = 1080$ mg).

Whereas sample 8 exhibited a unimodal and monodisperse size distribution characterized by a z-average and PDI values equal to 81 nm and 0.2 respectively, sample 7 displayed a multimodal size distribution with four populations (Figure 9). The first population (A, 3 nm) may correspond to the presence of SDS micelles[65, 66], the second and third populations (B, 28 nm and C, 190 nm) could be attributed to PHU nanoparticles and the fourth population (D, $> 2\mu\text{m}$) to PHU particle aggregates. The presence of these large aggregates was probably caused by depletion forces applied by SDS micelles [51, 73, 74]. The higher the number of micelles, the higher the depletion forces.

In order to evaluate the amount of SDS micelles in the samples, we determined the necessary quantity of SDS for covering the entire surface developed by the PHU nanoparticles (n_0), the amount of SDS providing the formation of the first micelle (n_{CMC}) according to Equations 5 – 8 (Table 3):

$$A_{tot} = \frac{6 \times m}{d \times \rho} \quad (5)$$

$$n_0 = \frac{A_{tot}}{A_0} \quad (6)$$

$$n = [SDS] \times V_w \quad (7)$$

$$n_{CMC} = CMC \times (V_{DMSO} + V_w) \quad (8)$$

With \mathbf{A}_{tot} the total surface of the PHU nanoparticles, \mathbf{m} the mass of PHU in the organic phase, \mathbf{d} the PHU nanoparticle size, $\mathbf{\rho}$ the density of PHU (1404 kg/m³), \mathbf{A}_0 the surface of PHU nanoparticle that can be covered by one SDS molecule, \mathbf{V}_{DMSO} the volume of DMSO (25 ml), \mathbf{CMC} the critical micellar concentration of SDS in the DMSO/water mixture. The detail of the calculations is presented in the supplementary information. The calculation of \mathbf{n}_0 was based on the hypothesis that the whole surface of the PHU nanoparticles was covered by a monolayer of SDS. The calculation of \mathbf{n}_{CMC} relied on the CMC of SDS determined in DMSO/water mixtures (1:2, 1:4 or 1:6 ratio) in the absence of PHU nanoparticles, assuming that DMSO entirely diffused toward the dispersing medium after nanoprecipitation.

The excess of SDS available to form micelles (\mathbf{n}^*) was then determined:

$$n^* = n - (n_0 + n_{CMC}) \quad (9)$$

With \mathbf{n} the SDS amount involved in the nanoprecipitation process.

For samples 5, 6, A, B, C and D, \mathbf{n}^* was inferior to \mathbf{n}_{CMC} , suggesting the absence of micelles which is consistent with the DLS curves exhibiting unimodal and monodisperse size distributions (Table 3). For samples 7 and 8, \mathbf{n}^* was superior to \mathbf{n}_{CMC} , providing the explanation of the presence of micelles observed by DLS as well as the multimodal size distribution and the presence of aggregates in sample 7 (Figure 9). However, with the same value of the \mathbf{n}^* to \mathbf{n}_{CMC} ratio as sample 7, sample 8 displayed a unimodal and monodisperse size distribution (PDI = 0.20, z-ave = 81 nm) and micelles were not observed. This difference may rely on the PHU concentration which was high for sample 8 (5 g/l) and low for sample 7 (1 g/l).

Influence of the amount of polymer

With V_{DMSO} , V_w and $[\text{SDS}]$ fixed, the coefficient analysis of response Y_1 revealed that the main effect of PHU concentration on the particle size (d) was negligible ($b_1 = -5.50 \text{ nm} < \Delta Y_2$, see Figure 4). Therefore, considering Equation 5, other parameters being equal, the increase of the PHU mass in the organic phase (m) (i.e. the increase of the PHU concentration) induced the increase of the total surface of the nanoparticles (A_{tot}) (samples 5 versus sample 6, sample 7 versus sample 8, Table 3). The higher A_{tot} , the lower the quantity of SDS available to form micelles, and the lower the concentration of micelles in the nanosuspension. This explains the differences observed between the size distributions displayed by samples 7 (polydisperse) and 8 (unimodal monodisperse).

At low water volume (50 ml) and high SDS concentration (25.0 mmol/l), it was found that the adjustment of PHU concentration could lead to either the lowest PDI (0.11, with $[\text{PHU}] = 5 \text{ g/l}$) or the lowest particle size (56 nm, with $[\text{PHU}] = 1 \text{ g/l}$). At fixed water volume and SDS concentration, the decrease of PHU concentration would lead to a more dilute regime [64] that enables a faster solvent-to-water diffusion [11, 58] and favors a lower particle growth time and nanoparticles with a lower size. Inversely, the increase of PHU concentration would induce the increase of A_{tot} , the decrease of the micelle concentration favoring a better particle stability right after the nanoprecipitation, and therefore a lower PDI.

Minimal size and minimal PDI

The DOE analysis pointed out that the lowest PDI was obtained with a high PHU concentration (5g/l), a low water volume (50 ml) and a high SDS concentration (25.0 mmol/l), while the lowest particle size was obtained with a low PHU concentration (1 g/l), a low water volume (50 ml) and a high SDS concentration (25.0 mmol/l) (Figure 7c) The corresponding responses calculated from the regression models (Equations 2 and 3) were equal to $\hat{Y}_1 = 0.11$ ($X_1 = +1, X_2 = -1, X_3 = +1$) and $\hat{Y}_2 = 56 \text{ nm}$ ($X_1 = -1, X_2 = -1, X_3 = +1$). These values were

close to the experimental responses in terms of PDI (sample 5: $z\text{-ave} = 55$ nm, PDI = 0.15) (Figure 10) or particle mean size (sample 6: $z\text{-ave} = 88$ nm, PDI = 0.10) (Figure 11), which highlighted the good predictive performance of the model used.

Runs 5 and 6 were repeated to assess the robustness of the PHU nanoprecipitation process (Figures 10 and 11).

The preparation of the smallest and most monodisperse PHU nanoparticles both required a low water volume (50 ml) and a high SDS concentration (25.0 mmol/l). This configuration corresponded to the adequate quantity of surfactant: small enough to cover the whole surface of the nanoparticles without inducing the formation of numerous micelles. The adjustment of the PHU concentration led either to the most monodisperse (5 g/l) or the smallest (1 g/l) nanoparticles. A high concentration of PHU led to the formation of more numerous PHU nanoparticles and tended to mitigate the destabilizing effect of SDS micelles. Consequently, the resulting nanosuspension was more monodisperse. On the other hand, a decrease of PHU concentration was accompanied by a decrease of the organic phase viscosity [64] and proto-particle growth time[18], resulting in the production of smaller nanoparticles.

Based on theoretical calculations and nanoprecipitation experiments (using PCL, acetone and polyvinylalcohol as a polymer, organic solvent and surfactant respectively), Lebouille et al. suggested that the smallest nanoparticles could be obtained with an excess of surfactant [75]. This result is contradictory to those obtained for PHU nanoprecipitation.

Ageing study

Samples were stored at 24°C and submitted to DLS analyses 17, 27, 47 and 214 days after their preparation (Table 4).

Samples A, B and C – corresponding to the centre points – appeared the more stable since they exhibited 214 days after their preparation a PDI between 0.11 and 0.14 and no significant

size variation. Sample 6 ([PHU] = 5 g/l, V_w = 50 ml, [SDS] = 25.0 mmol/l) – exhibiting the lowest initial PDI value (0.10) – remained stable with a PDI value remaining low (0.13) in spite of a slight increase of particle mean size (from 88 to 113 nm) between $t = 0$ and $t = 17$ d. These results suggested that a low PDI initial value should favor the stability of NP over time in accordance with the results of Beck-Broichsitter[14] and Zhang [71]. Destabilization of sample 5 ([PHU] = 1 g/l, V_w = 50 ml, [SDS] = 25.0 mmol/l) – lowest particle size (55 nm) – began at $t = 47$ d with a PDI value above 0.2. The sample was totally aggregated at $t = 214$ d (PDI = 0.91, d_{moy} = 104 nm). One can explain these results by the excess of SDS (n^*) and the low PHU concentration. These results highlighted that low particle mean size does not guarantee nanosuspension stability over time.

The samples prepared without SDS (samples 1, 2, 3 and 4) rapidly exhibited significant size distribution fluctuations over time leading to complete aggregation after 214 days (PDI > 0.7). These results proved the necessary presence of SDS to delay the destabilization of the PHU nanosuspension. Nevertheless, for high SDS concentration (25mM), the nanosuspension stability appeared dependent on PHU concentration. Sample 7 ([PHU] = 1 g/l, V_w = 150 ml, [SDS] = 25.0 mmol/l) was directly destabilized after its preparation, whereas the destabilization of sample 8 ([PHU] = 5 g/l; V_w = 150 ml, [SDS] = 25.0 mmol/l) was observed after 17 days. These results pointed out the negative effect of the micelle presence on the nanoparticle stability.

To conclude, SDS was mandatory for delaying the destabilization of PHU nanosuspension, but SDS concentration must be fixed according to both PHU concentration and water volume, in agreement with the 3-factor interaction effect (b_{123}) value (Figure 4).

Cryo-TEM observations

Some PHU nanoparticles were analyzed by cryo-TEM. Sample B ([PHU] = 3 g/l, V_w = 100 ml, [SDS] = 12.5 mmol/l) (centre point), sample 6 ([PHU] = 5 g/l, V_w = 50 ml, [SDS] = 25.0

mmol/l) (lowest PDI), sample 4 ([PHU] = 5 g/l, V_w = 150 ml, [SDS] = 0.0 mmol/l) (surfactant-free sample) and sample 8 ([PHU] = 5 g/l, V_w = 150 ml, [SDS] = 25.0 mmol/l) (sample prepared with high SDS concentration) were observed by cryo-TEM at various time after their preparation (Figures 12, 13 and 14 respectively). Small spherical spots with low contrast correspond to PHU nanoparticles (Figure 12) while small black dots with high contrast (Figure 13) correspond to frost. Very few nanoparticles can be observed on the images because of the very low volume of the suspension droplet deposited on the carbon film (0.45 μ l) as well as very low PHU concentration (0.14 to 1.67 g/l).

Cryo-TEM observations confirmed DLS results. Beside nanoparticles with diameter between 200 and 300 nm, Figures 13a and 13b show two particles with significantly higher size: one particle measured 1 μ m (Figure 13a) while another one measured 400 nm (Figure 13b) (red circles). These two objects have a less neat outline than the other particles suggesting that they were swollen by DMSO. Nanoparticles of sample 8 with diameter around 70 nm (Figure 14a and 14b) appear aggregated in varying size cluster (200 to 700 nm). This observation is consistent with the DLS curve (Figure S4).

Despite the precautions taken to protect nanoparticles from the electron beam (cryo-TEM MET method, accelerating voltage of 120 kV, condenser lenses adjusted to spot n^o5), zooms caused nanoparticle degradations, sometimes in just a few seconds (progressive bleaching observed in Figure S3). Such examples of polymer degradation caused by the TEM electron beam have been previously reported [76, 77]. In the case of the PHU nanoparticles, the energy transferred by the electron beam probably broke weak chemical bindings (e.g. inter- and intramolecular hydrogen bindings) and deteriorated the cohesion between the macromolecules forming the nanoparticles.

Conclusion

The preparation of PHU nanoparticle by nanoprecipitation was optimized using a full-factorial design to point out the influence of experimental parameters on particle size distribution. The lowest PDI (0.10) was obtained with a PHU concentration of 5 g/l, a water volume of 50ml and an SDS concentration of 25.0 mmol/l, while the lowest particle size (55 nm) was obtained with a PHU concentration of 1 g /l, a water volume of 50ml and an SDS concentration of 25.0 mmol/l.

These experimental results were very close to the corresponding responses calculated from the developed regression models ($\hat{Y}_1 = 0.11$ and $\hat{Y}_2 = 56$ nm), which underlines their good predictive performance. The regression coefficient analysis allowed evidencing the more significant parameters and pointing out the crucial interaction effects on the nanoparticle size distribution.

The presence of SDS was mandatory to prevent PHU nanoparticles from aggregating, provided that the quantity of SDS available to form micelles was inferior to the CMC, since the presence of micelles destabilized the nanosuspensions.

At a fixed value of water volume and SDS concentration, PHU concentration governed the value of the total surface developed by the nanoparticles and was crucial for the formation of SDS micelles. The latter induced the aggregation of PHU nanoparticles through depletion forces. A low PHU concentration corresponding to a more dilute regime in the organic phase enabled the formation of smaller nanoparticles but may induce the presence of micelles. The increase of PHU concentration may limit the formation of micelles in the nanoparticle dispersing medium, and thus improve the nanosuspension stability over time.

The ageing study revealed that nanosuspensions with the lowest PDI (≈ 0.1) were stable for more than seven months. PDI was therefore the most determining factor for nanoparticle stability on the long term. On the contrary, samples containing either no surfactant or numerous SDS micelles were rapidly destabilized.

Cryo-TEM observations confirmed the DLS results. Spherical and monodisperse nanoparticles were observed for samples offering low PDI. In absence of surfactant, the nanoparticles appeared more polydisperse, whereas the effect of micelle depletion forces in samples prepared with an excess of SDS was evidenced by the observation of micrometer-sized clusters.

Acknowledgements

We thank P. Alcouffe (UMR CNRS 5223, IMP) for TEM experiments at the Technological Centre of Microstructures of University Lyon1.

Supporting Information. Brief statement in nonsentence format listing the content of the material supplied as Supporting Information.

References:

- [1] R. Lochhead, V. Padman, L. Anderson, L.A. Wilgus, P. McDaniel, L. LaBeaud, K. Davis, E. Hoff, J. Epler, Skin care polymer IP trends, *Household Pers. Prod. Ind.*, 47 (2010) 71-76.
- [2] B. Perlatti, P.L.d.S. Bergo, M.F.d.G. Fernandes da Silva, J.B. Fernandes, M.R. Forim, Polymeric nanoparticle-based insecticides: a controlled release purpose for agrochemicals, *InTech*, 2013, pp. 521-548.
- [3] K.M. El-Say, H.S. El-Sawy, Polymeric nanoparticles: Promising platform for drug delivery, *Int. J. Pharm. (Amsterdam, Neth.)*, 528 (2017) 675-691.
- [4] R. Gref, Y. Minamitake, M.T. Peracchia, V. Trubetskoy, V. Torchilin, R. Langer, Biodegradable long-circulating polymer nanospheres, *Science (Washington, D. C., 1883-)*, 263 (1994) 1600-1603.
- [5] E. Allemann, R. Gurny, E. Doelker, Preparation of aqueous polymeric nanodispersions by a reversible salting-out process: influence of process parameters on particle size, *Int. J. Pharm.*, 87 (1992) 247-253.
- [6] C. Perez, A. Sanchez, D. Putnam, D. Ting, R. Langer, M.J. Alonso, Poly(lactic acid)-poly(ethylene glycol) nanoparticles as new carriers for the delivery of plasmid DNA, *J. Controlled Release*, 75 (2001) 211-224.
- [7] A. Shariati, C.J. Peters, Recent developments in particle design using supercritical fluids, *Curr. Opin. Solid State Mater. Sci.*, 7 (2003) 371-383.
- [8] Y. Toshio, H. Mitsuru, M. Shozo, S. Hitoshi, Specific delivery of mitomycin c to the liver, spleen and lung: Nano- and microspherical carriers of gelatin, *International Journal of Pharmaceutics*, 8 (1981) 131-141.
- [9] C.P. Reis, R.J. Neufeld, A.J. Ribeiro, F. Veiga, Design of insulin-loaded alginate nanoparticles: influence of the calcium ion on polymer gel matrix properties, *Chem. Ind. Chem. Eng. Q.*, 12 (2006) 47-52.
- [10] S. Anandhakumar, M. Sasidharan, C.-W. Tsao, A.M. Raichur, Tailor-Made Hollow Silver Nanoparticle Cages Assembled with Silver Nanoparticles: An Efficient Catalyst for Epoxidation, *ACS Appl. Mater. Interfaces*, 6 (2014) 3275-3281.
- [11] S. Gatti, A. Agostini, R. Ferrari, D. Moscatelli, Synthesis and nanoprecipitation of HEMA-CLn based polymers for the production of biodegradable nanoparticles, *Polymers (Basel, Switz.)*, 9 (2017) 389/381-389/314.
- [12] F. Lince, D.L. Marchisio, A.A. Barresi, Strategies to control the particle size distribution of poly- ϵ -caprolactone nanoparticles for pharmaceutical applications, *J. Colloid Interface Sci.*, 322 (2008) 505-515.
- [13] H. Fessi, F. Puisieux, J.P. Devissaguet, N. Ammoury, S. Benita, Nanocapsule formation by interfacial polymer deposition following solvent displacement, *Int. J. Pharm.*, 55 (1989) R1-R4.
- [14] M. Beck-Broichsitter, J. Nicolas, P. Couvreur, Solvent selection causes remarkable shifts of the "Ouzo region" for poly(lactide-co-glycolide) nanoparticles prepared by nanoprecipitation, *Nanoscale*, 7 (2015) 9215-9221.

- [15] C.E. Mora-Huertas, H. Fessi, A. Elaissari, Polymer-based nanocapsules for drug delivery, *Int J Pharm*, 385 (2010) 113-142.
- [16] E. Lepeltier, C. Bourgaux, P. Couvreur, Nanoprecipitation and the "Ouzo effect": Application to drug delivery devices, *Adv. Drug Delivery Rev.*, 71 (2014) 86-97.
- [17] S. Galindo-Rodriguez, E. Allemann, H. Fessi, E. Doelker, Physicochemical Parameters Associated with Nanoparticle Formation in the Salting-Out, Emulsification-Diffusion, and Nanoprecipitation Methods, *Pharm. Res.*, 21 (2004) 1428-1439.
- [18] C.E. Mora-Huertas, H. Fessi, A. Elaissari, Influence of process and formulation parameters on the formation of submicron particles by solvent displacement and emulsification-diffusion methods, *Adv. Colloid Interface Sci.*, 163 (2011) 90-122.
- [19] D. Quintanar-Guerrero, E. Allemann, H. Fessi, E. Doelker, Preparation techniques and mechanisms of formation of biodegradable nanoparticles from preformed polymers, *Drug Dev. Ind. Pharm.*, 24 (1998) 1113-1128.
- [20] J. Molpeceres, M. Guzman, M.R. Aberturas, M. Chacon, L. Berges, Application of Central Composite Designs to the Preparation of Polycaprolactone Nanoparticles by Solvent Displacement, *Journal of Pharmaceutical Sciences*, 85 (1996) 206-213.
- [21] A. Bozkir, O.M. Saka, Formulation and investigation of 5-FU nanoparticles with factorial design-based studies, *Farmaco*, 60 (2005) 840-846.
- [22] V.M. Pandya, J.K. Patel, D.J. Patel, Formulation, optimization and characterization of simvastatin nanosuspension prepared by nanoprecipitation technique, *Pharm. Lett.*, 3 (2011) 129-140.
- [23] Y. Singh, P. Ojha, M. Srivastava, M.K. Chourasia, Reinvestigating nanoprecipitation via Box-Behnken design: a systematic approach, *J Microencapsul*, 32 (2015) 75-85.
- [24] A. Piras, A. Dessy, M. Alderighi, S. Sandreschi, C. Federica, Doxorubicin Loaded Polyurethanes Nanoparticles, *NanoBiomedEng*, 4 (2012) 83-88.
- [25] H. Fu, H. Gao, G. Wu, Y. Wang, Y. Fan, J. Ma, Preparation and tunable temperature sensitivity of biodegradable polyurethane nanoassemblies from diisocyanate and poly(ethylene glycol), *Soft Matter*, 7 (2011) 3546-3552.
- [26] M.D. Lelah, L.K. Lambrecht, B.R. Young, S.L. Cooper, Physicochemical characterization and in vivo blood tolerability of cast and extruded Biomer, *J. Biomed. Mater. Res.*, 17 (1983) 1-22.
- [27] R. Chandra, R. Rustgi, Biodegradable polymers, *Prog. Polym. Sci.*, 23 (1998) 1273-1335.
- [28] A. Valerio, S.R.P. da Rocha, P.H.H. Araujo, C. Sayer, Degradable polyurethane nanoparticles containing vegetable oils, *Eur. J. Lipid Sci. Technol.*, 116 (2014) 24-30.
- [29] L. Torini, J. Argillier, N. Zydowicz, Interfacial polycondensation encapsulation in miniemulsion, *Macromolecules*, 38 (2005) 3225-3236.
- [30] A. Schoth, K. Landfester, R. Munoz-Espi, Surfactant-Free Polyurethane Nanocapsules via Inverse Pickering Miniemulsion, *Langmuir*, 31 (2015) 3784-3788.
- [31] M.H. Karol, J.A. Kramarik, Phenyl isocyanate is a potent chemical sensitizer, *Toxicol. Lett.*, 89 (1996) 139-146.
- [32] S. Gupta, R. Upadhyaya, Cancer and p21 protein expression: in relation with isocyanate toxicity in cultured mammalian cells, *Int. J. Pharm. Res. Bio-Sci.*, 3 (2014) 20-28.

- [33] W.F. Diller, Pathogenesis of phosgene poisoning, *Toxicol. Ind. Health*, 1 (1985) 7-15.
- [34] L. Maisonneuve, O. Lamarzelle, E. Rix, E. Grau, H. Cramail, Isocyanate-Free Routes to Polyurethanes and Poly(hydroxy Urethane)s, *Chem. Rev. (Washington, DC, U. S.)*, 115 (2015) 12407-12439.
- [35] C. Carre, L. Bonnet, L. Averous, Original biobased nonisocyanate polyurethanes: solvent- and catalyst-free synthesis, thermal properties and rheological behavior, *RSC Adv.*, 4 (2014) 54018-54025.
- [36] C. Hahn, H. Keul, M. Moeller, Hydroxyl-functional polyurethanes and polyesters: synthesis, properties and potential biomedical application, *Polym. Int.*, 61 (2012) 1048-1060.
- [37] B. Ochiai, S. Inoue, T. Endo, One-pot non-isocyanate synthesis of polyurethanes from bisepoxide, carbon dioxide, and diamine, *J. Polym. Sci., Part A: Polym. Chem.*, 43 (2005) 6613-6618.
- [38] H. Tomita, F. Sanda, T. Endo, Model reaction for the synthesis of polyhydroxyurethanes from cyclic carbonates with amines: substituent effect on the reactivity and selectivity of ring-opening direction in the reaction of five-membered cyclic carbonates with amine, *J. Polym. Sci., Part A: Polym. Chem.*, 39 (2001) 3678-3685.
- [39] T. Quérette, E. Fleury, N. Sintès-Zydowicz, Non-isocyanate polyurethane nanoparticles prepared by nanoprecipitation, *European Polymer Journal*, 114 (2019) 434-445.
- [40] G.E. Box, J.S. Hunter, W.G. Hunter, *Statistics for experimenters*, Wiley Series in Probability and Statistics, Wiley Hoboken, NJ2005.
- [41] K. Derakhshandeh, M. Erfan, S. Dadashzadeh, Encapsulation of 9-nitrocamptothecin, a novel anticancer drug, in biodegradable nanoparticles: factorial design, characterization and release kinetics, *European journal of pharmaceuticals and biopharmaceutics*, 66 (2007) 34-41.
- [42] B. Gourdon, C. Chemin, A. Moreau, T. Arnaud, P. Baummy, S. Cisternino, J.-M. Péan, X. Declèves, Functionalized PLA-PEG nanoparticles targeting intestinal transporter PepT1 for oral delivery of acyclovir, *International journal of pharmaceuticals*, 529 (2017) 357-370.
- [43] C. Draheim, F. de Crécy, S. Hansen, E.-M. Collnot, C.-M. Lehr, A design of experiment study of nanoprecipitation and nano spray drying as processes to prepare PLGA nano- and microparticles with defined sizes and size distributions, *Pharmaceutical research*, 32 (2015) 2609-2624.
- [44] J. Saadé, C. Bordes, G. Raffin, M. Hangouët, P. Marote, K. Faure, Response surface optimization of miniemulsion: application to UV synthesis of hexyl acrylate nanoparticles, *Colloid and Polymer Science*, 294 (2016) 27-36.
- [45] M. Sabapati, N.N. Palei, R.B. Molakpogu, Solid lipid nanoparticles of *Annona muricata* fruit extract: formulation, optimization and in vitro cytotoxicity studies, *Drug development and industrial pharmacy*, 45 (2019) 577-586.
- [46] R.G. LeBel, D.A.I. Goring, Density, viscosity, refractive index, and hygroscopicity of mixtures of water and dimethyl sulfoxide, *J. Chem. Eng. Data*, 7 (1962) 100-101.
- [47] C. Wohlfarth, Dielectric constant of the mixture (1) water;(2) dimethylsulfoxide, *Supplement to IV/6*, Springer2008, pp. 524-526.
- [48] F. Gaudin, N. Sintès-Zydowicz, Poly(urethane-urea) nanocapsules prepared by interfacial step polymerisation in miniemulsion, *Colloids Surf., A*, 384 (2011) 698-712.

- [49] H.D. Lu, K.D. Ristroph, E.L.K. Dobrijevic, J. Feng, S.A. McManus, Y. Zhang, W.D. Mulhearn, H. Ramachandruni, A. Patel, R.K. Prud'homme, Encapsulation of OZ439 into Nanoparticles for Supersaturated Drug Release in Oral Malaria Therapy, *ACS Infect Dis*, (2018).
- [50] A.L. Boehm, I. Martinon, R. Zerrouk, E. Rump, H. Fessi, Nanoprecipitation technique for the encapsulation of agrochemical active ingredients, *J. Microencapsulation*, 20 (2003) 433-441.
- [51] J. Bibette, D. Roux, B. Pouligny, Creaming of emulsions: the role of depletion forces induced by surfactant, *J. Phys. II*, 2 (1992) 401-424.
- [52] H. Ma, M. Luo, L.L. Dai, Influences of surfactant and nanoparticle assembly on effective interfacial tensions, *Phys. Chem. Chem. Phys.*, 10 (2008) 2207-2213.
- [53] P. Wydro, The miscibility of sodium dodecyl sulfonate with anionic, nonionic and cationic surfactants in mixed monolayers and micelles, *Pol. J. Chem.*, 81 (2007) 2157-2169.
- [54] L.R. Harutyunyan, S.A. Markarian, Investigation of the effect of dimethyl sulfoxide and diethyl sulfoxide on sodium dodecyl sulfate micellization in aqueous solutions by fluorescence method, *Colloid J.*, 69 (2007) 407-410.
- [55] P.S. Christoffer Johans, Delta-8 multichannel microtensiometer: Influence of DMSO on the CMC of SDS, Technical note, Kibron Inc., 2004.
- [56] M.J. Rosen, J.T. Kunjappu, *Micelle Formation by Surfactants, Surfactants and Interfacial Phenomena*, John Wiley & Sons, Inc.2012, pp. 123-201.
- [57] H. Schott, Extent of hydration of dimethyl sulfoxide in aqueous solution, *J. Pharm. Sci.*, 58 (1969) 946-948.
- [58] Z. Lu, E. Manias, M. Lanagan, D.D. MacDonald, Dielectric relaxation in dimethyl sulfoxide/water mixtures, *ECS Trans.*, 28 (2010) 11-21.
- [59] M.J. Schick, A.H. Gilbert, Effect of urea, guanidinium chloride, and dioxane on the c.m.c. [critical micelle concentration] of branched-chain nonionic detergents, *J. Colloid Sci.*, 20 (1965) 464-472.
- [60] C. Contado, E. Vighi, A. Dalpiaz, E. Leo, Influence of secondary preparative parameters and aging effects on PLGA particle size distribution: a sedimentation field flow fractionation investigation, *Anal. Bioanal. Chem.*, 405 (2013) 703-711.
- [61] Y. Dong, S.-S. Feng, Methoxy poly(ethylene glycol)-poly(lactide) (MPEG-PLA) nanoparticles for controlled delivery of anticancer drugs, *Biomaterials*, 25 (2004) 2843-2849.
- [62] M. Chorny, I. Fishbein, H.D. Danenberg, G. Golomb, Lipophilic drug loaded nanospheres prepared by nanoprecipitation: effect of formulation variables on size, drug recovery and release kinetics, *J. Controlled Release*, 83 (2002) 389-400.
- [63] O. Thioune, H. Fessi, J.P. Devissaguet, F. Puisieux, Preparation of pseudolatex by nanoprecipitation: Influence of the solvent nature on intrinsic viscosity and interaction constant, *Int. J. Pharm.*, 146 (1997) 233-238.
- [64] P. Legrand, S. Lesieur, A. Bochot, R. Gref, W. Raatjes, G. Barratt, C. Vauthier, Influence of polymer behaviour in organic solution on the production of polylactide nanoparticles by nanoprecipitation, *Int. J. Pharm.*, 344 (2007) 33-43.

- [65] C. Fonseca, S. Simoes, R. Gaspar, Paclitaxel-loaded PLGA nanoparticles: preparation, physicochemical characterization and in vitro anti-tumoral activity, *J. Controlled Release*, 83 (2002) 273-286.
- [66] H. Asadi, K. Rostamizadeh, D. Salari, M. Hamidi, Preparation of biodegradable nanoparticles of tri-block PLA-PEG-PLA copolymer and determination of factors controlling the particle size using artificial neural network, *J. Microencapsulation*, 28 (2011) 406-416.
- [67] A. Arizaga, G. Ibarz, R. Pinol, Stimuli-responsive poly(4-vinyl pyridine) hydrogel nanoparticles: Synthesis by nanoprecipitation and swelling behavior, *J. Colloid Interface Sci.*, 348 (2010) 668-672.
- [68] C. Giannavola, C. Bucolo, A. Maltese, D. Paolino, M.A. Vandelli, G. Puglisi, V.H.L. Lee, M. Fresta, Influence of preparation conditions on acyclovir-loaded poly-d,l-lactic acid nanospheres and effect of PEG coating on ocular drug bioavailability, *Pharm. Res.*, 20 (2003) 584-590.
- [69] F. Ganachaud, J.L. Katz, Nanoparticles and nanocapsules created using the Ouzo effect: spontaneous emulsification as an alternative to ultrasonic and high-shear devices, *ChemPhysChem*, 6 (2005) 209-216.
- [70] S. Hirsjaervi, L. Peltonen, J. Hirvonen, Surface pressure measurements in particle interaction and stability studies of poly(lactic acid) nanoparticles, *Int. J. Pharm.*, 348 (2008) 153-160.
- [71] C. Zhang, V.J. Pansare, R.K. Prud'homme, R.D. Priestley, Flash nanoprecipitation of polystyrene nanoparticles, *Soft Matter*, 8 (2012) 86-93.
- [72] T. Riley, T. Govender, S. Stolnik, C.D. Xiong, M.C. Garnett, L. Illum, S.S. Davis, Colloidal stability and drug incorporation aspects of micellar-like PLA-PEG nanoparticles, *Colloids Surf., B*, 16 (1999) 147-159.
- [73] Student, The probable error of a mean, *Biometrika*, 6 (1908) 1-25.
- [74] J. Borkowski, *Response Surface Methodology: Process and Product Optimization Using Designed Experiments* (3rd ed.). by Raymond H. Myers, Douglas C. Montgomery, and Christine M. Anderson-Cook, *J. Am. Stat. Assoc.*, 105 (2010) 879.
- [75] J.G.J.L. Lebouille, R. Stepanyan, J.J.M. Slot, M.A. Cohen Stuart, R. Tuinier, Nanoprecipitation of polymers in a bad solvent, *Colloids Surf., A*, 460 (2014) 225-235.
- [76] J. Cheng, Formulation of functionalized PLGA-PEG nanoparticles for in-vitro targeted drug delivery, *Biomaterials*, 28 (2007) 869-876.
- [77] N.Sintes-Zydowicz, G. Gaudin, Core-shell Biocompatible Polyurethane Nanocapsules obtained by Interfacial Step Polymerisation in Miniemulsion, *Colloids and Surfaces A*, 331 (2008) 133-142.

Caption for figures

Figure 1. Main effects and interaction coefficients for response Y_1 (PDI).

Figure 2. Two-way diagrams representing the interaction effects X_2X_3 (a) and X_1X_3 (b) for response Y_1 (PDI)

Figure 3. Maps of the interaction effects between X_1 , X_2 , X_3 for response Y_1 (PDI) with $X_3 = -1$ (a) and $X_3 = +1$ (b) ($X_1 = [\text{PHU}]$, $X_2 = V_w$, $X_3 = [\text{SDS}]$).

Figure 4. Main effects and interaction coefficients for response Y_2 (particle size).

Figure 5. Maps of the interaction effects between X_2 and X_3 (a), X_1 and X_2 (b), for response Y_2 (particle size) ($X_1 = [\text{PHU}]$, $X_2 = V_w$, $X_3 = [\text{SDS}]$).

Figure 6. Maps of the interaction effects between X_1 , X_2 , X_3 for response Y_2 (particle size) with $X_3 = -1$ (a) and $X_3 = +1$ (b) ($X_1 = [\text{PHU}]$, $X_2 = V_w$, $X_3 = [\text{SDS}]$).

Figure 7. Contour plot of the response surface showing the effect of PHU concentration (X_1) and water volume on the particle size (Y_2) at different SDS concentrations (X_3) ([SDS] = 0 mmol/l (a), [SDS] = 12.5 mmol/l (b), [SDS] = 25.0 mmol/l (c)).

Figure 8. Nanoparticle size distribution for sample 1 ([PHU] = 1 g/l, $V_w = 50$ ml, [SDS] = 0.0 mmol/l).

Figure 9. Nanoparticle size distribution for sample 7 ([PHU] = 1 g/l, $V_w = 150$ ml, [SDS] = 25.0 mmol/l).

Figure 10. Nanoparticle size distribution for samples 5 and 5' ([PHU] = 1 g/l, $V_w = 50$ ml, [SDS] = 25.0 mmol/l).

Figure 11. Nanoparticle size distribution for samples 6, 6' and 6'' ([PHU] = 5 g/l, $V_w = 50$ ml, [SDS] = 25.0 mmol/l).

Figure 12. Cryo-TEM images of sample B ([PHU] = 3 g/l, $V_w = 100$ ml, [SDS] = 12.5 mmol/l) after 55 days (a) and sample 6 ([PHU] = 5 g/l, $V_w = 50$ ml, [SDS] = 25.0 mmol/l) after 57 days (b). black arrows indicate frost dots

Figure 13. Cryo-TEM images of sample 8 ([PHU] = 5 g/l, $V_w = 150$ ml, [SDS] = 25.0 mmol/l) after 57 days.

Figure 1

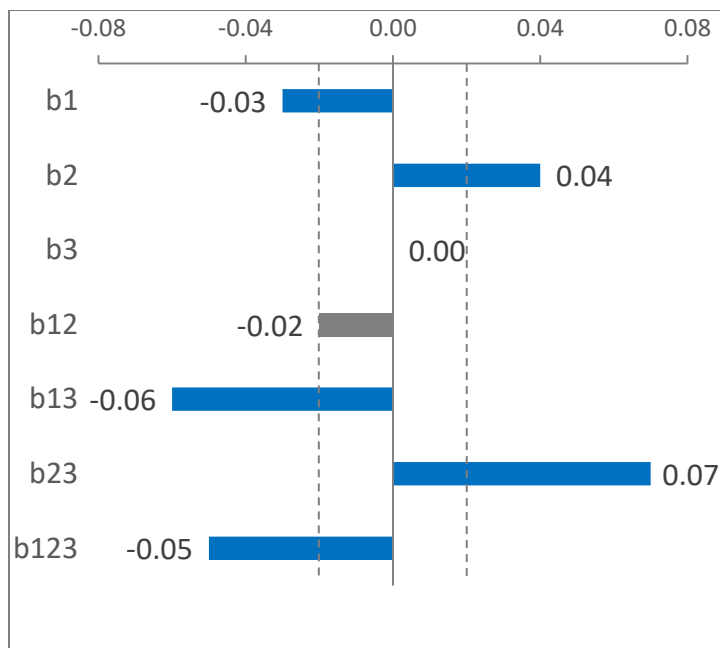


Figure 2

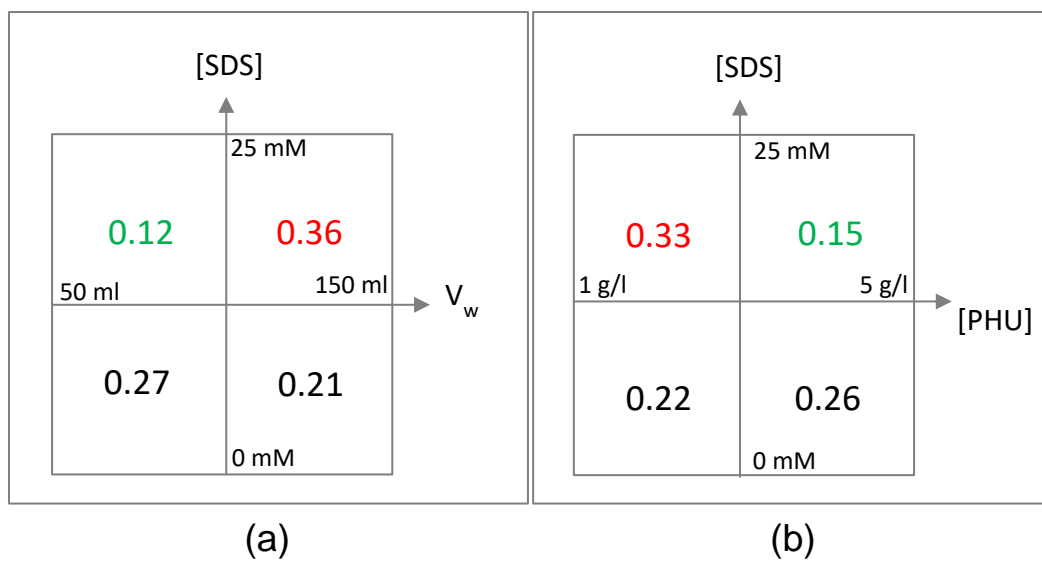


Figure 3

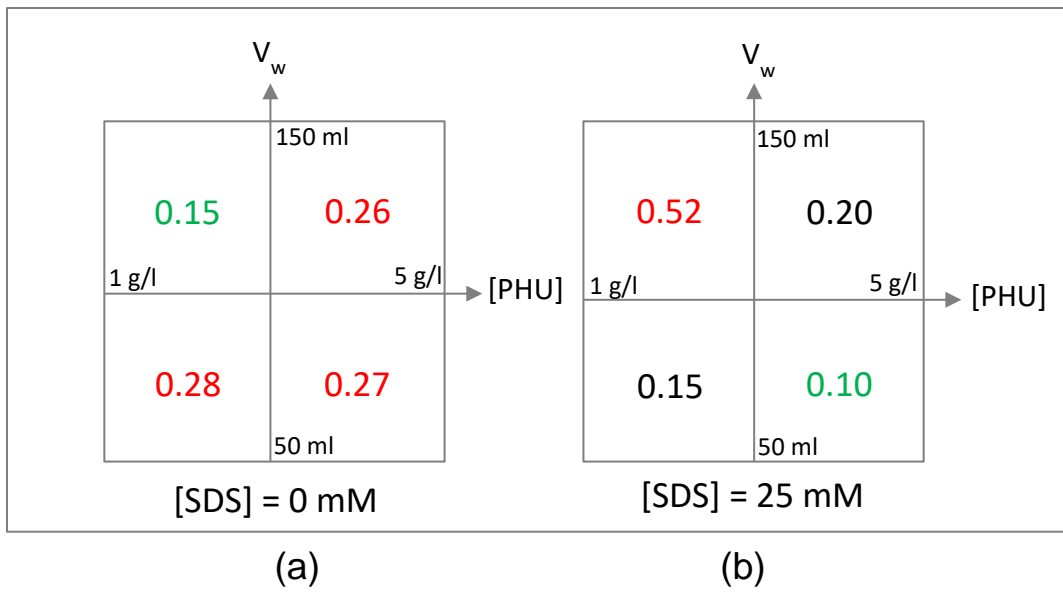


Figure 4

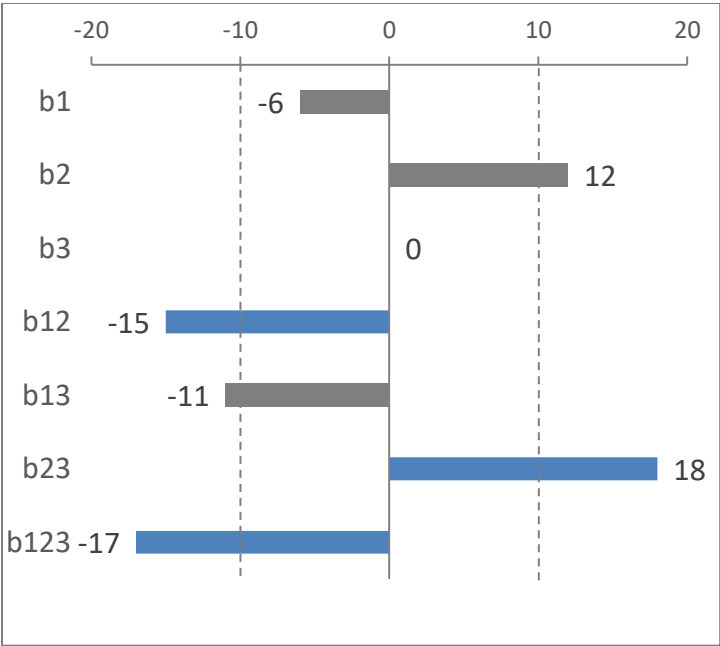


Figure 5

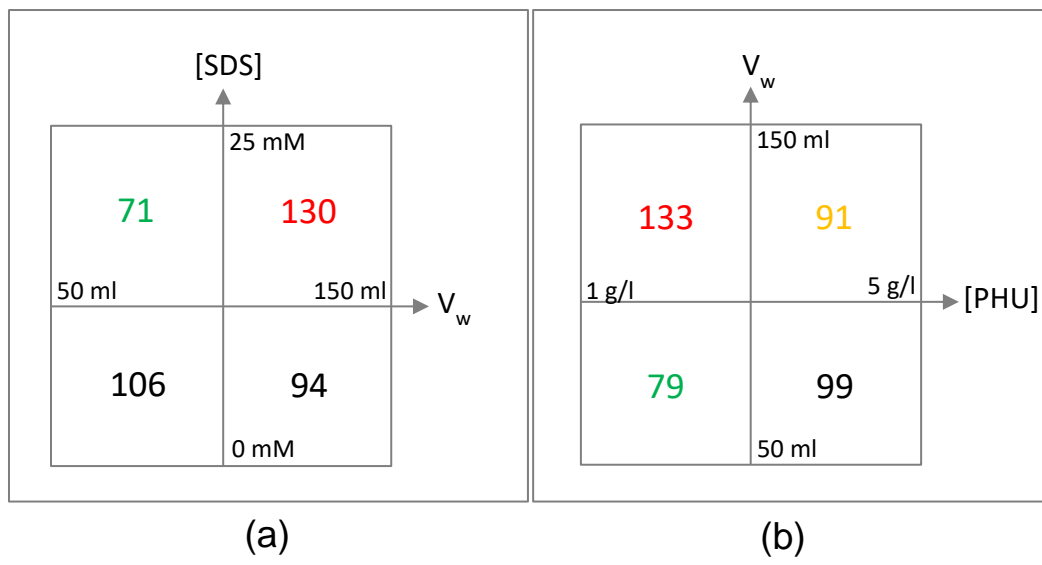


Figure 6

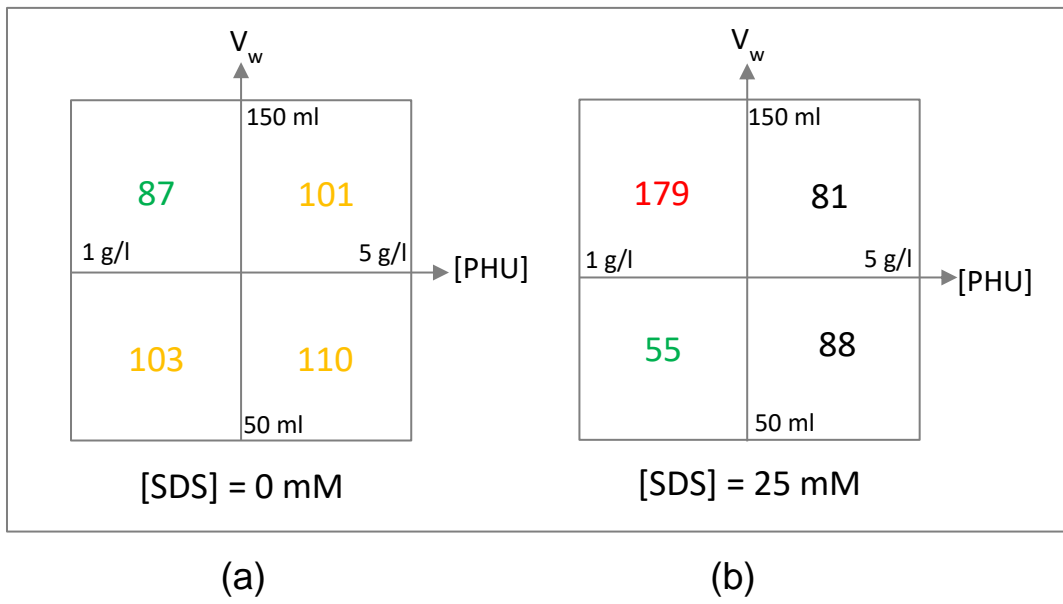


Figure 7

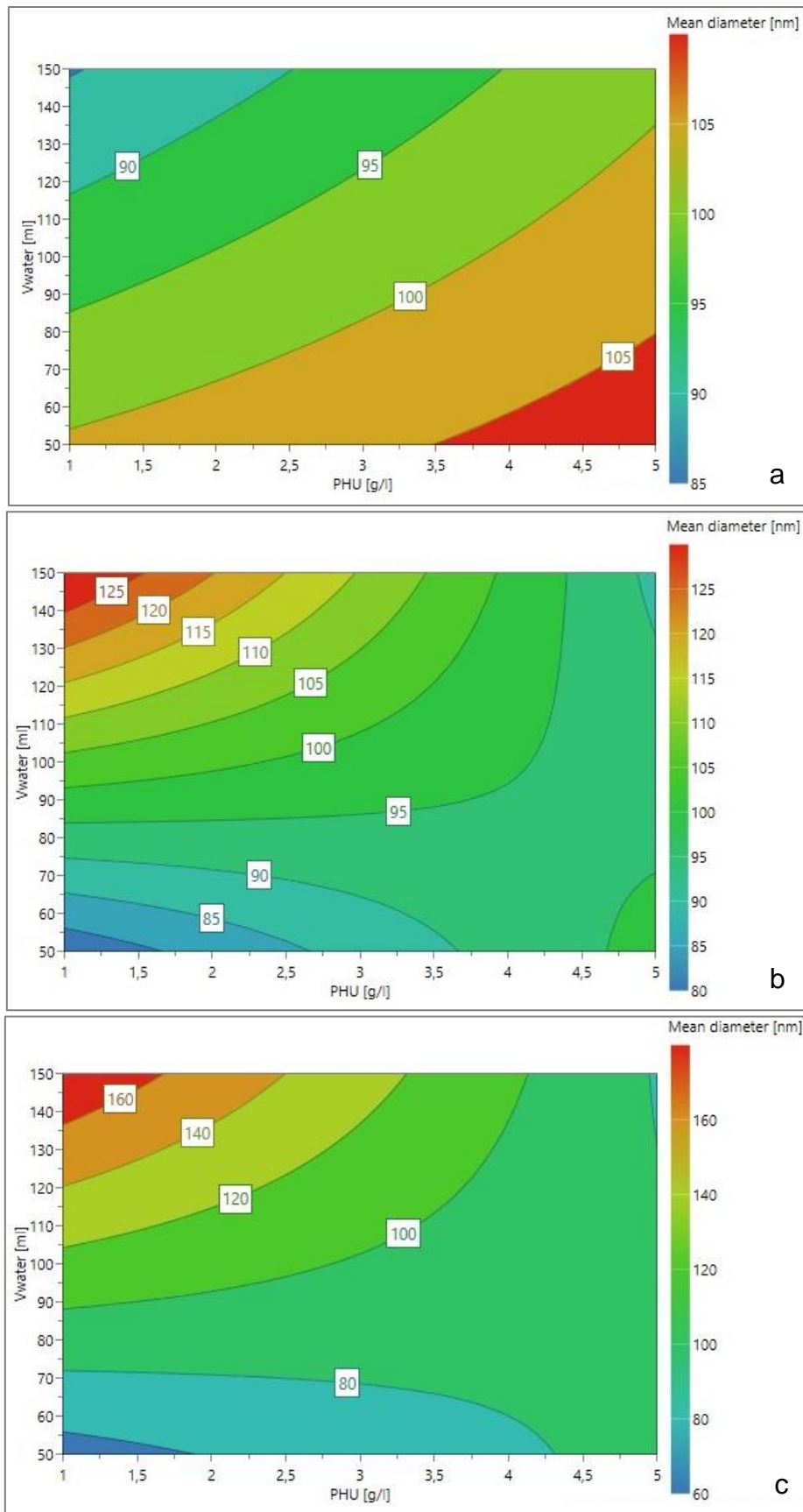


Figure 8

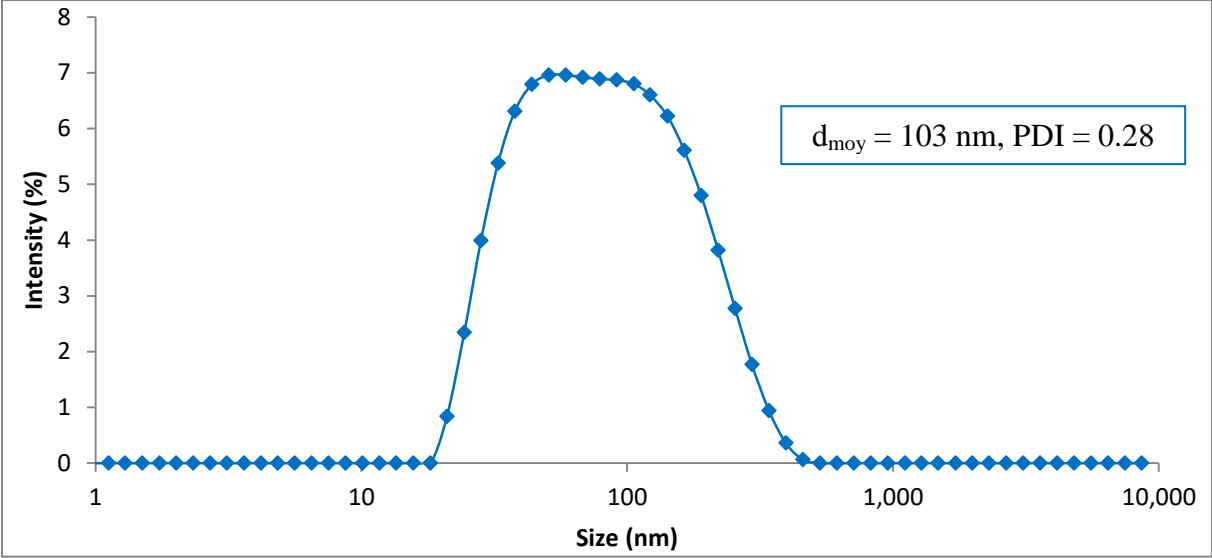


Figure 9

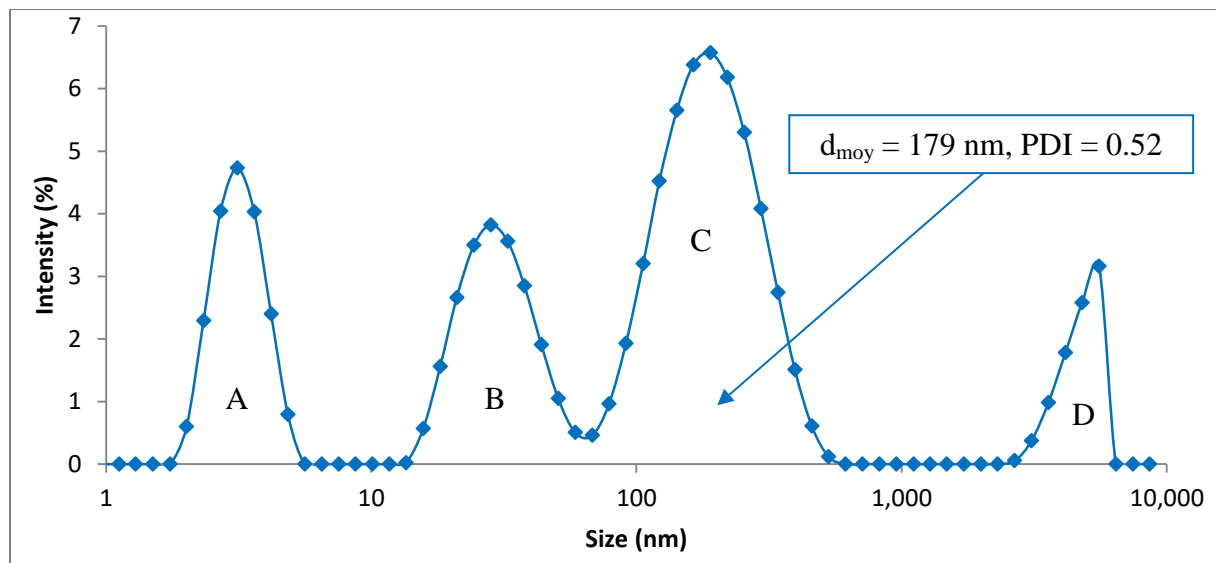


Figure 10

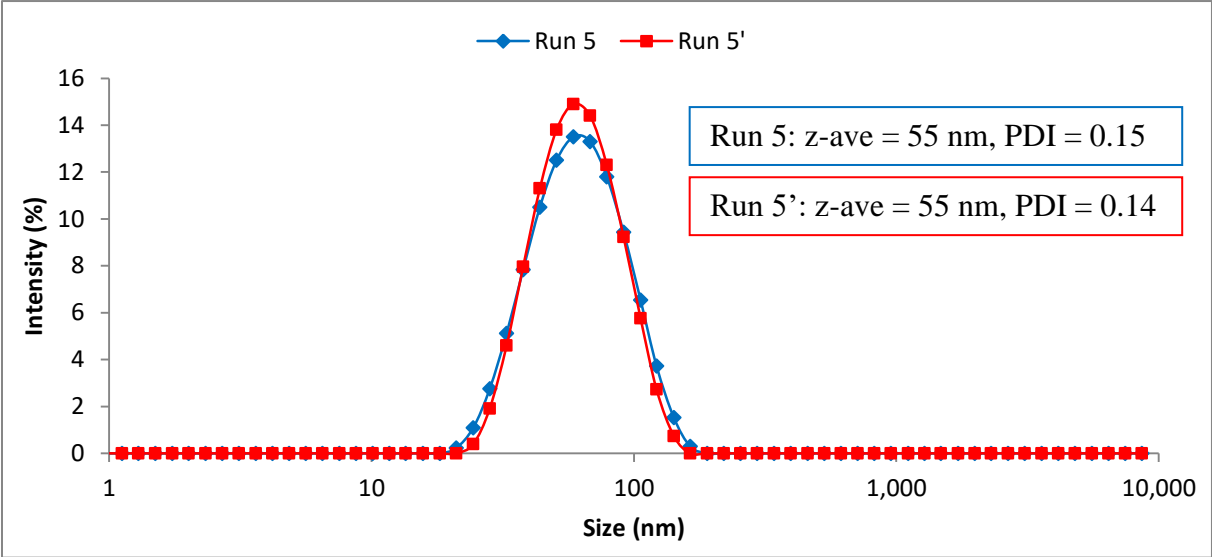


Figure 11

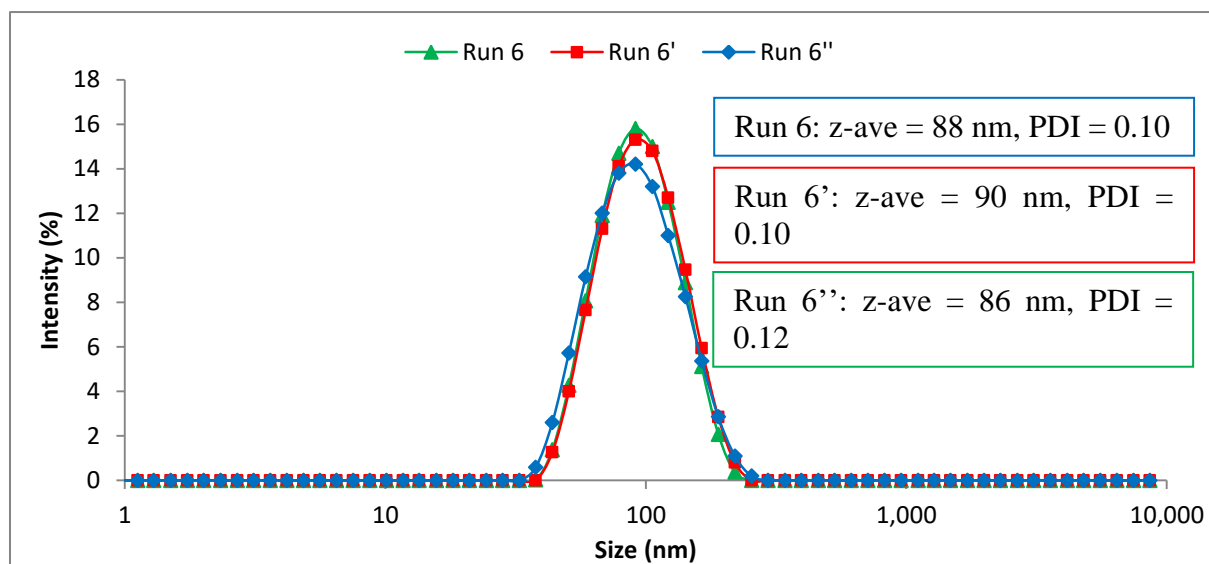


Figure 12

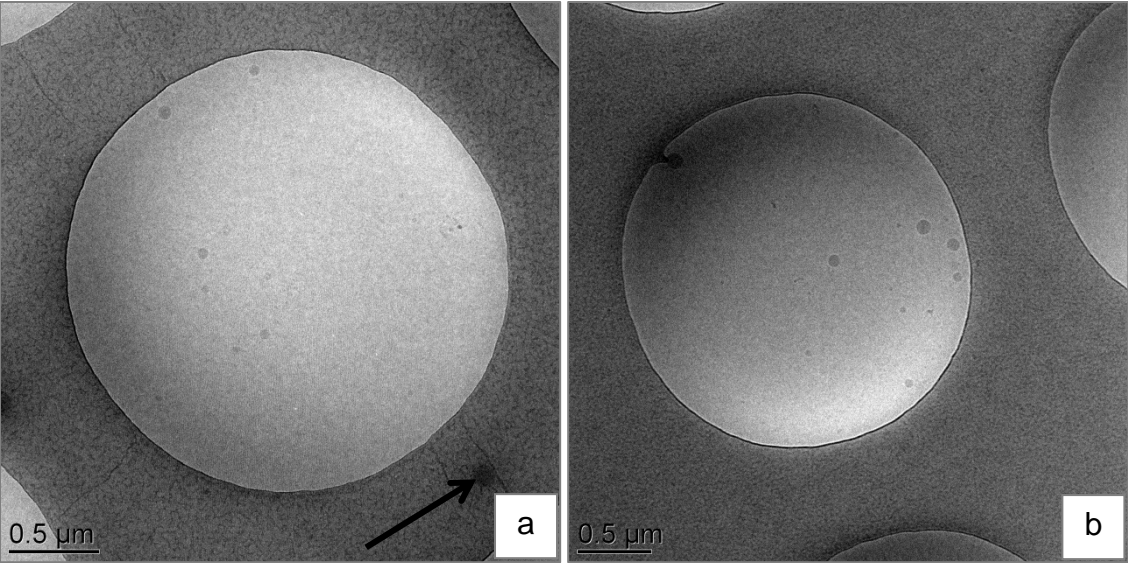


Figure 13

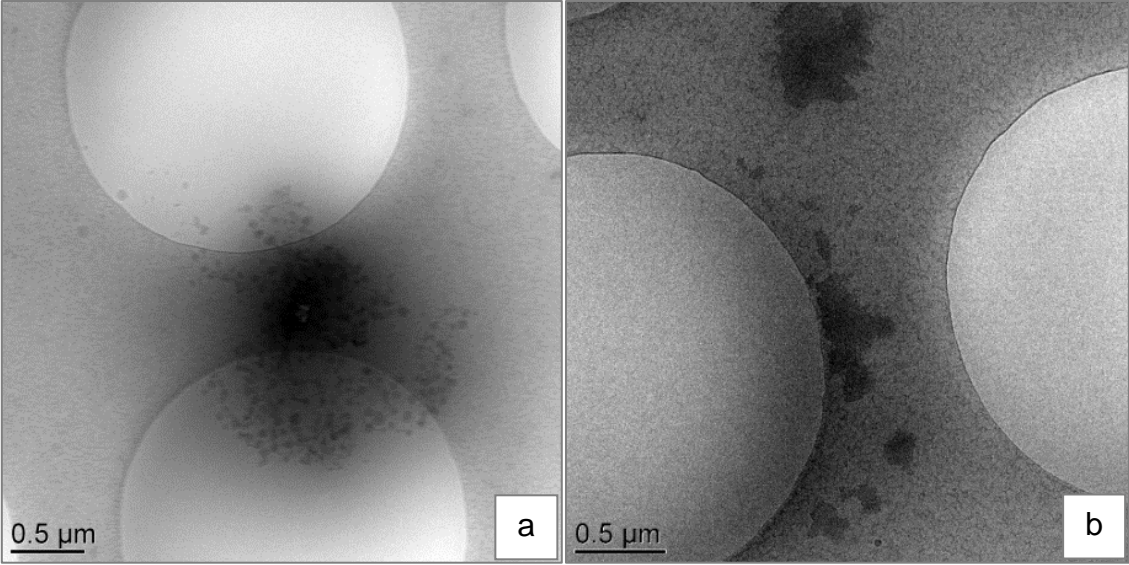


Table 1: Full-factorial matrix and experimental results.

	Run	Coded variable			Natural variable			Response	
		X ₁	X ₂	X ₃	[PHU]	V _w	[SDS]	Y ₁ (PDI)	Y ₂ (d)
Cube edges	1	-1	-1	-1	1	50	0.0	0.28	103
	2	1	-1	-1	5	50	0.0	0.27	110
	3	-1	1	-1	1	150	0.0	0.15	87
	4	1	1	-1	5	150	0.0	0.26	101
	5	-1	-1	1	1	50	25.0	0.15	55
	6	1	-1	1	5	50	25.0	0.10	88
	7	-1	1	1	1	150	25.0	0.52	179
	8	1	1	1	5	150	25.0	0.20	81
Centre points	A	0	0	0	3	100	12.5	0.12	102
	B	0	0	0	3	100	12.5	0.13	86
	C	0	0	0	3	100	12.5	0.13	93
	D	0	0	0	3	100	12.5	0.13	93
Repeated runs	3'	-1	1	-1	1	150	0.0	0.20	88
	3''	-1	1	-1	1	150	0.0	0.25	118
	4'	1	1	-1	5	150	0.0	0.28	137
	4''	1	1	-1	5	150	0.0	0.29	110
	5'	-1	-1	1	1	50	25.0	0.14	55
	6'	1	-1	1	5	50	25.0	0.10	90
	6''	1	-1	1	5	50	25.0	0.12	86
					g/l	ml	mmol/l		nm

Bold figures: unimodal and polydisperse (PDI > 0.2) size distributions.

Red figures: multimodal and polydisperse size distributions.

PDI ≤ 0.2 ⇒ d = z-ave ; PDI > 0.2 ⇒ d = d_{moy}

Table 2: Main effects and interaction coefficients for responses Y_1 (PDI) and Y_2 (particle size)

Effects	b_0	b_1	b_2	b_3	b_{12}	b_{13}	b_{23}	b_{123}
Y_1	0.24	-0.03	0.04	0.00	-0.02	-0.06	0.07	-0.05
Y_2	101	-6	12	0	-15	-11	18	-17

Table 3: Necessary quantity of SDS for covering the entire surface (A_{tot}) developed by the PHU nanoparticles (n_0), amount of SDS providing the formation of the first micelle (n_{cmc}), excess of SDS available to form micelles (n^*) for the DoE samples containing SDS

Sample	Parameter			Response		A_{tot}	n_0 (mol)	N (mol)	n_{cmc} (mol)	n^* (mol)	n_{cmc} / n^*
	m_{PHU} (g)	V_w (ml)	[SDS] (M)	PDI	d						
5	25	50	25	0.15	55	1.94	1.02×10^{-5}	1.25×10^{-3}	7.95×10^{-4}	4.45×10^{-4}	1,79
6	125	50	25	0.10	88	6.07	3.20×10^{-5}	1.25×10^{-3}	7.95×10^{-4}	4.23×10^{-4}	1,88
7	25	150	25	0.52	179	0.60	2.46×10^{-6}	3.75×10^{-3}	1.17×10^{-3}	2.58×10^{-3}	0,46
8	125	150	25	0.2	81	6.60	2.72×10^{-5}	3.75×10^{-3}	1.17×10^{-3}	2.55×10^{-3}	0,46
A	75	100	12.5	0.12	102	3.14	1.27×10^{-5}	1.25×10^{-3}	9.75×10^{-4}	2.62×10^{-4}	3,72
B	75	100	12.5	0.13	86	3.73	1.50×10^{-5}	1.25×10^{-3}	9.75×10^{-4}	2.60×10^{-4}	3,75
C	75	100	12.5	0.13	93	3.45	1.39×10^{-5}	1.25×10^{-3}	9.75×10^{-4}	2.61×10^{-4}	3,73
D	75	100	12.5	0.13	93	3.45	1.39×10^{-5}	1.25×10^{-3}	9.75×10^{-4}	2.61×10^{-4}	3,73
	mg	ml	mmol/l		nm	m ²	mol	mol	mol	mol	

Red figures: multimodal and polydisperse size distributions.

$PDI \leq 0.2 \Rightarrow d = z\text{-ave}$; $PDI > 0.2 \Rightarrow d = d_{moy}$

Table 4: Evolution of the samples size and size distribution over time.

Run	X ₁	X ₂	X ₃	d	PDI	d	PDI	d	PDI	d	PDI	d	PDI
				nm		nm		nm		nm		nm	
	Age (days)			0		17		27		47		214	

Centre points

A	3	100	12.5	102	0.12	97	0.12	97	0.11	98	0.13	97	0.14
B	3	100	12.5	86	0.13	80	0.12	81	0.12	80	0.12	82	0.14
C	3	100	12.5	93	0.13	85	0.13	85	0.13	86	0.12	87	0.13

Sample with the lowest PDI

6	5	50	25	88	0.10	113	0.13	111	0.14	106	0.13	103	0.16
---	---	----	----	----	------	-----	------	-----	------	-----	------	-----	------

Sample with the lowest particle size

5	1	50	25	55	0.15	59	0.14	60	0.15	77	0.22	104	0.91
---	---	----	----	----	------	----	------	----	------	-----------	-------------	------------	-------------

Samples without surfactant

1	1	50	0	103	0.28	105	0.23	94	0.18	119	0.05	262	1
2	5	50	0	110	0.27	97	0.17	99	0.17	117	0.06	227	0.75
3	1	150	0	87	0.15	602	0.29	160	1	183	0.87	298	1
4	5	150	0	101	0.26	90	0.12	144	0.04	427	0.03	259	0.99

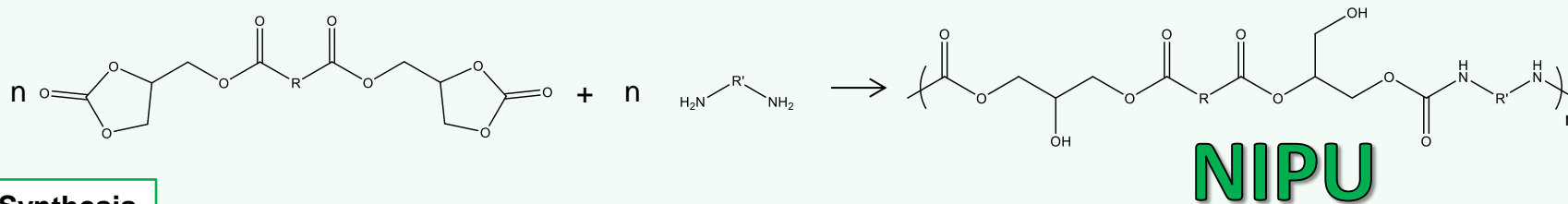
Samples with an excess of surfactant

7	1	150	25	179	0.52	152	0.35	105	0.48	113	0.19	136	0.27
8	5	150	25	81	0.2	85	0.89	115	0.99	100	0.6	81	0.39

Bold figures: unimodal and polydisperse size distributions.

Red figures: multimodal and polydisperse size distributions.

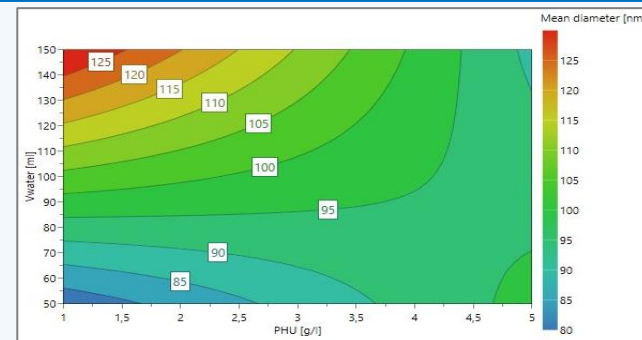
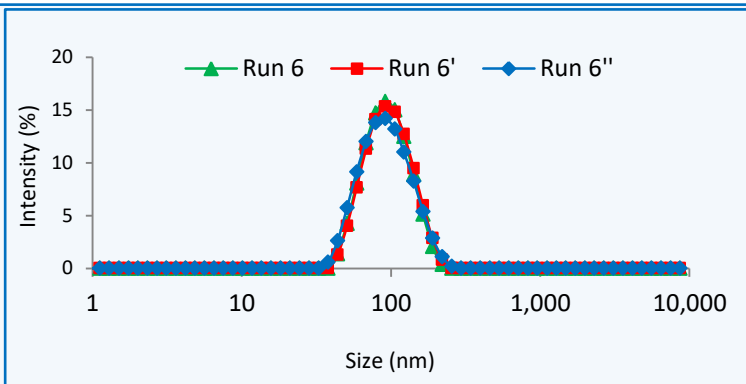
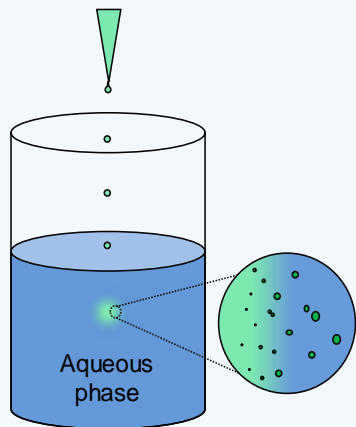
$PDI \leq 0.2 \Rightarrow d = z\text{-ave}$; $PDI > 0.2 \Rightarrow d = d_{\text{moy}}$



1. Synthesis

2. Nanoprecipitation Optimization

Organic phase
(NIPU + solvent)



**NIPU
nanoparticles**

